

# Attenuation of high-frequency body waves in the crust of the Central External Dinarides

Iva Dasović · Marija Ruščić · Davorka Herak · Marijan Herak

Received: 13 February 2015 / Accepted: 13 May 2015 / Published online: 27 May 2015  
© Springer Science+Business Media Dordrecht 2015

**Abstract** The Central External Dinarides are known as a tectonically complex region of moderate seismicity where several strong earthquakes occurred in the last century. In order to gain insight into the attenuation of seismic waves in the area, the extended coda normalization method was applied to band-pass-filtered seismograms of local earthquakes recorded at seven seismological broadband stations. Obtained results indicate strong attenuation of direct body waves:  $Q_{0,P}=Q_P(1\text{ Hz})$  is found between 21 and 120 and  $Q_{0,S}=Q_S(1\text{ Hz})$  is between 46 and 113, whereas the exponent  $n$  in the power law of frequency dependence of the quality factor is found in the range of 0.63–1.52 and 0.65–0.97 for  $n_P$  and  $n_S$ , respectively. P-waves are, on the average, attenuated more than S-waves. The three island stations (Dugi Otok (DUGI), Žirje (ZIRJ), Hvar (HVAR)) are distinguished by the strong low-frequency P-wave attenuation and more pronounced frequency dependence of the  $Q_P$  factor ( $Q_{0,S}/Q_{0,P}>1.7$ ,  $Q_{0,P}<60$ ,

$n_P>n_S$ ). The remaining four inland stations (Udbina (UDBI), Morići (MORI), Kijevo (KIJV), Čačvina (CACV)) all exhibit similar qualitative attenuation properties for P- and S-waves ( $n_P\approx n_S\approx 1$  and  $Q_{0,S}\approx Q_{0,P}$ ), although individual values of the  $Q$ -factors vary notably within this group. Low-frequency attenuation of direct S-waves in the crust is stronger than mean attenuation of scattered coda waves in the lithosphere, especially for long coda lapse times. The results are also qualitatively in agreement with the thermal regime in the area.

**Keywords** Body waves · Attenuation · Coda normalization method · Crust · Dinarides · Croatia

## 1 Introduction

Attenuation is an important parameter needed to retrieve seismic source properties, to estimate moment magnitude and ground motion characteristics and to assess seismic hazard. It reflects the process of seismic waves' energy loss as they propagate through inelastic and heterogeneous media that results in amplitude decrease; moreover, it reflects medium's properties. Inelasticity causes conversion of elastic energy into heat; this intrinsic absorption is caused mainly by small-scale crystal dislocations, interstitial fluids and frictional heating. Attenuation due to the heterogeneity, however, redistributes energy through scattering on all sorts of variations in physical characteristics of rocks (faults, cracks, intrusions, small-scale irregularities, etc.). Discrimination of these two effects is not a simple task (Sato et al. 2012),

---

I. Dasović (✉) · M. Ruščić · D. Herak · M. Herak (✉)  
Andrija Mohorovičić Geophysical Institute, Department of  
Geophysics, Faculty of Science, University of Zagreb,  
Horvatovac 95, 10000 Zagreb, Croatia  
e-mail: dasovici@gfz.hr  
e-mail: mherak@gfz.hr

M. Ruščić  
e-mail: ruscic@geophysik.uni-kiel.de

D. Herak  
e-mail: dherak@gfz.hr

M. Ruščić  
Institute of Geoscience, Christian-Albrechts-University of  
Kiel, Ludewig-Meyn-Str. 10, 24118 Kiel, Germany

but for practical use, there is often no need for separating intrinsic and scattering attenuation, as mostly the total attenuation is of interest (Havskov and Ottemöller 2010).

Attenuation is usually described by the quality factor  $Q$ , a measure of the energy loss per cycle. Depending on the type of seismic waves that are considered, we distinguish attenuation of S-waves ( $Q_S^{-1}$ ), P-waves ( $Q_P^{-1}$ ), coda waves ( $Q_C^{-1}$ ), etc. In order to estimate direct S-wave attenuation, Aki (1980) developed empirical coda normalization method applicable to one station only. Yoshimoto et al. (1993) extended it to direct P-waves. The method is based on the proportionality of source spectral amplitudes of body waves and the coda waves, which enables the elimination of seismic source effect in direct waves by normalization with observed coda wave's amplitudes. This procedure also removes site effects, leaving only the factor of attenuation.

The Central External Dinarides (CED) is one of the most active areas in the Dinarides where several strong earthquakes occurred in the last 150 years; hence, the seismic hazard level is one of the highest in Croatia and its neighbouring countries (Herak et al. 2011). The area is tectonically very complex with the Moho topography varying rapidly from the Adriatic microplate towards the Dinarides, where Stipčević et al. (2011) and Stipčević (2012) found indications of a very thick crust. However, the structure and geodynamics of the Dinarides are very complex and insufficiently understood.

For the region of the External Dinarides and its adjacent area, Herak (1991) and Dasović et al. (2012, 2013) analyzed attenuation of coda waves applying the modified coda- $Q$  method (Aki and Chouet 1975). These studies found the coda waves' attenuation to be very strong. Attenuation of coda waves reflects the average attenuation of the lithosphere, whereas attenuation of the direct seismic phases of shallow local earthquakes depicts the properties of the crust, mostly its upper layers. As no attempt has been made so far to infer attenuation properties of direct waves in the CED, we address this important issue by applying the extended coda normalization method to local earthquakes recorded at seven seismological stations. Insight into spatial distribution of seismic attenuation within the crust should provide additional information on the properties of the main tectonic units there. At the same time, the results will hopefully enable more reliable modelling of propagation and source effects for local earthquakes.

## 2 Tectonic setting and seismic activity

The area of our interest is a part of the complex Alpine–Carpathian–Dinaric orogenic system. It is characterized by interaction of the Adriatic microplate, the Dinarides and the Pannonian basin (Tomljenović et al. 2008; Ustaszewski et al. 2008 and references therein). Due to the push of the African plate, the Adriatic microplate collides with the European plate and underthrusts the Dinarides to the northeast resulting in a broad thrust and fold belt.

According to Tomljenović et al. (2008), the External Dinarides are derived from the Adriatic microplate and are composed of Mesozoic to Tertiary shallow-marine carbonate platform formations (limestone, dolomites, breccias, etc.). Palaeogene shortening is considered to be the main deformational phase which resulted in characteristic NW trend and SW vergence of compressional and imbricated structures. The adjacent Internal Dinarides are situated to the northeast of the External Dinarides; they are composed of several tectonic units with dominant NW–SE trend (flysch, ophiolite and suture zone) (for more details, look in Tomljenović et al. 2008; Ustaszewski et al. 2008 and references therein).

The area of the CED lies in the part where the Mohorovičić discontinuity is the deepest: using receiver function method Stipčević et al. (2011) and Stipčević (2012) estimated the depth of the Moho larger than 40 km, under some stations even deeper than 50 km. The crust is the thickest along the External Dinarides next to the Internal Dinarides and it thins out in the perpendicular directions to NE and SW. The crust is three layered: the upper crust is up to 28 km thick (e.g. models for the stations KIJV and Čačvina (CACV) in Stipčević et al. 2011) with carbonate sediments of up to 11 km of thickness, possibly even more.

The belt of the highest seismic activity in the External Dinarides extends south-eastwards from Mt. Dinara to the areas of Imotski, Ston, Dubrovnik and farther to the Montenegrin coast (Fig. 1). The area is characterized by reverse faults, striking predominantly in the NW–SE and W–E directions, and some strike-slip faulting mostly in the hinterland (Ivančić et al. 2006; Kuk et al. 2000). The majority of earthquakes occur in the upper crust, not deeper than 20–25 km. Seismicity is moderate to high with rare occurrence of strong events,

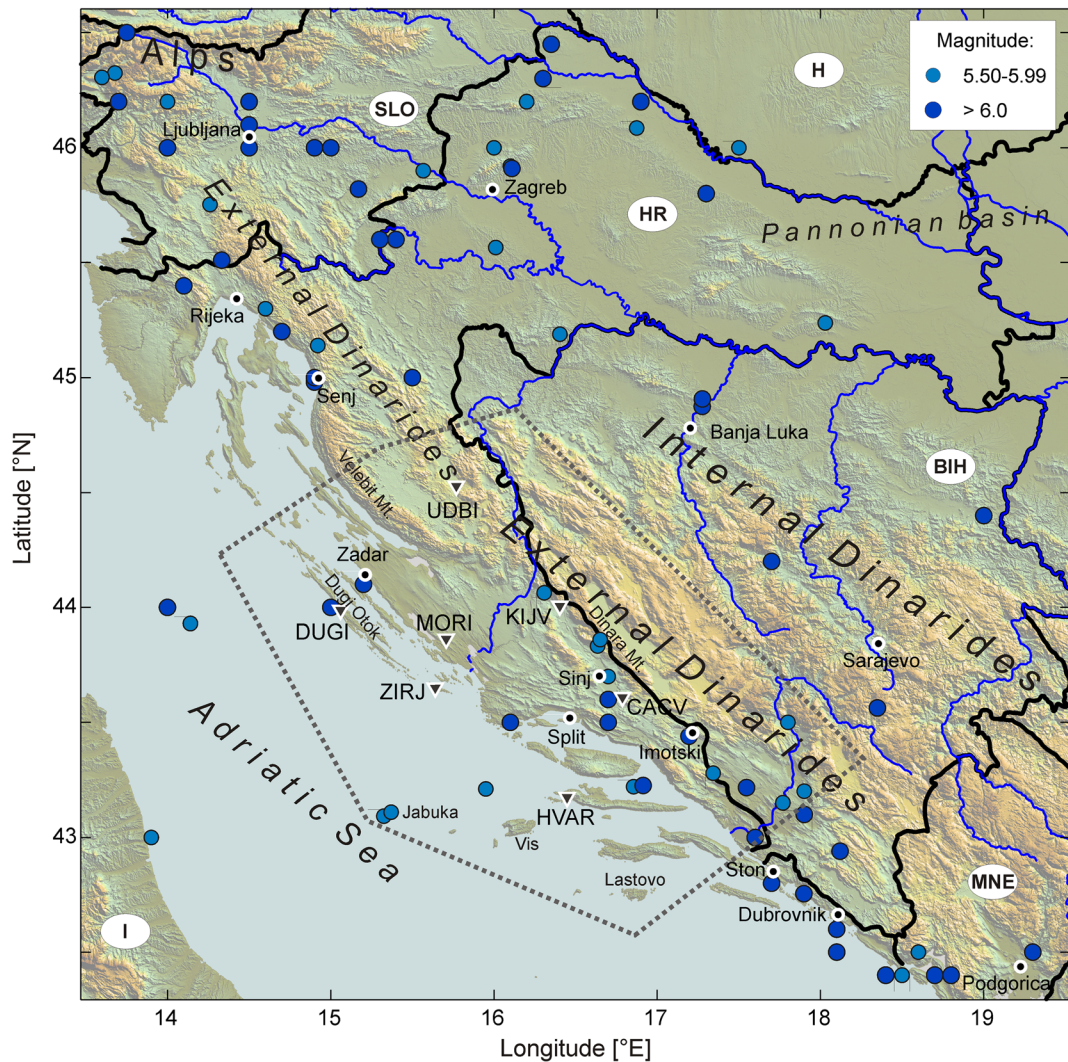


**Fig. 1** Studied area in the geographical context. Triangles mark seismological stations used in the analysis, and dotted lines roughly delineate the region of our interest. Historical seismicity ( $M_L \geq 5.5$ ) after Croatian Earthquake Catalogue (updated version described in Herak et al. 1996) is shown by solid circles

and it is intensified towards southeast. Croatian Earthquake Catalogue (Herak et al. 1996; updated with events up to 2013) includes 16 earthquakes with  $M_L \geq 5.5$  in the studied area of the CED (dotted-line polygon in Fig. 1) in the last 150 years. The strongest was the one of 2 July 1898 near Sinj with  $I_0 = IX$  °MCS ( $M_L = 6.7$ ; Markušić and Herak 1999). The strongest event in Croatia in the twentieth century occurred on 29 December 1942 near Imotski with  $M_L = 6.2$  and  $I_0 = VIII-IX$  °MCS.

There is also notable seismic activity in the Central Adriatic area. Most of the earthquakes there occur in the vicinity of Jabuka Island, a large

eruptive intrusion. Many earthquakes used in the analysis for the Hvar (HVAR) station are, in fact, the aftershocks of the 29 March 2003 17:42 mainshock ( $M_L = 5.5$ ) of the Jabuka earthquakes series, which was analyzed in detail by Herak et al. (2005). This epicentral area is located W and NW of Jabuka Island. Seismic profiles indicate the presence of reverse structures extending to the SE.

Seismic activity is also prominent at fault systems along Dugi Otok Island and Mt. Velebit. In the Velebit region, the largest instrumentally recorded earthquake was the one of 1916 ( $M_L = 5.8$ ,  $I_0 = VIII$  °MCS) near Senj.

### 3 Method and data analysis

#### 3.1 Method

In order to estimate attenuation of high-frequency S-waves, we used the coda normalization method proposed by Aki (1980) and its extension to P-waves suggested by Yoshimoto et al. (1993). The coda normalization method is a purely empirical technique based on observations that the ratio of source spectral amplitudes of S-waves,  $A_S(f)$ , and spectral amplitudes of coda waves,  $A_C(f, t)$ , depends only on distance, i.e. time  $t$ , and on the radiation pattern. Yoshimoto et al. (1993) showed that this holds also for source spectral amplitudes of P-waves,  $A_P(f)$ . This means that the source effect can be eliminated by normalizing S- and P-wave spectral amplitudes with coda spectral amplitudes measured at a fixed time ( $t_C$ ). The effect of radiation pattern is removed by averaging the ratio over many events. Local site effects are also removed by this normalization because coda waves are scattered S-waves and because the ratio of the effects for S-waves and P-waves is constant. This gives us relations

$$\ln \frac{A_P(f)r}{A_C(f, t_C)} = -\frac{\pi f}{Q_P(f)v_P}r + \text{const.} \quad (1a)$$

$$\ln \frac{A_S(f)r}{A_C(f, t_C)} = -\frac{\pi f}{Q_S(f)v_S}r + \text{const.} \quad (1b)$$

where  $r$  represents hypocentral distance,  $v_P$  and  $v_S$  are average seismic velocities of direct phases and  $Q_P$  and  $Q_S$  are quality factors for P- and S-waves, respectively. By applying linear regressions following Eqs. (1a) and (1b) to the observed data triplets  $[A_{P,S}(f), A_C(f, t_C), r]$  and assuming appropriate average seismic velocities, the quality factors can be obtained from the slope of the regression line.

Quality factors for P- and S-waves are frequency dependent. This dependence is usually well described by a simple power law

$$Q(f) = Q_0 f^n \Rightarrow \ln Q(f) = \ln Q_0 + n \ln f, \quad (2)$$

where  $Q_0$  is either  $Q_{0,P}=Q_P(f=1 \text{ Hz})$  or  $Q_{0,S}=Q_S(f=1 \text{ Hz})$ .  $Q_{0,P}$ ,  $Q_{0,S}$  and frequency dependence exponents  $n_P$  and  $n_S$  are estimated by linear regression (for more detailed description, please see, e.g. Aki 1980; Yoshimoto et al. 1993; and Sato et al. 2012).

#### 3.2 Data

The analyzed seismograms of local earthquakes were recorded by seven seismological broadband stations from the Croatian seismograph network: Udbina (UDBI), Kijevo (KIJV), Čačvina (CACV), Morići (MORI), Dugi Otok (DUGI), Žirje (ZIRJ) and HVAR (Fig. 2), managed by the Croatian Seismological Survey (see Table 1 for detail).

A total of 1199 seismograms of 817 local earthquakes with epicentral distances between 40 and 120 km and local magnitude larger or equal to 2.0 were used. All earthquakes are shallow with source depth mostly down to 15 km, i.e. in the uppermost crust. Epicentres of the analyzed earthquakes are shown in Fig. 2.

#### 3.3 Data analysis

To obtain spectral amplitudes, we firstly detrended all three components of the seismogram and applied Butterworth band-pass filter of the fourth order for up to 12 central frequencies ( $f=1.5, 2, 3, 4, 5, 6, 8, 9, 12, 16, 18, 24 \text{ Hz}$ ) with the bandwidth of  $2f/3$ , depending on the sampling frequency  $f_S$  (Table 1). Then, we calculated the signal as root mean square of the total velocity of the wave field defined as

$$v_{T,RMS}(t_n) = \sqrt{\frac{1}{N} \sum_{n-\frac{N}{2}}^{n+\frac{N}{2}} v_Z^2(t_n) + v_{NS}^2(t_n) + v_{EW}^2(t_n)}$$

where  $t_n$  is the time of the  $n^{\text{th}}$  sample measured from the earthquake origin time and  $N=2f_S/f+1$  is the length of sample for which mean is calculated. The noise level, defined as the mean of a 5-s-long window of  $v_{T,RMS}$  preceding the P-wave onset, was then subtracted from the whole signal.  $A_P(f)$  and  $A_S(f)$  were taken as the maxima of the signal in the 5-s-long windows starting at the onset of P- and S-waves, respectively (Fig. 3).  $A_C(f, t_C)$  is taken as a mean value of the signal of a 5-s-long window starting at  $t_C=55 \text{ s}$  after earthquake origin time. We used only well-recorded seismograms for which signal to noise ratio (SNR) for P-, S- and coda waves were greater than 2.

We chose earthquakes with source–receiver distances up to 120 km, for which the  $P_g$  and  $S_g$  phases dominate in the first 5 s of the P- and S-wavetrains; therefore, estimates of the  $Q$ -factors mostly describe attenuation properties of the upper layers of the crust. Chosen  $t_C=55 \text{ s}$  ensures that

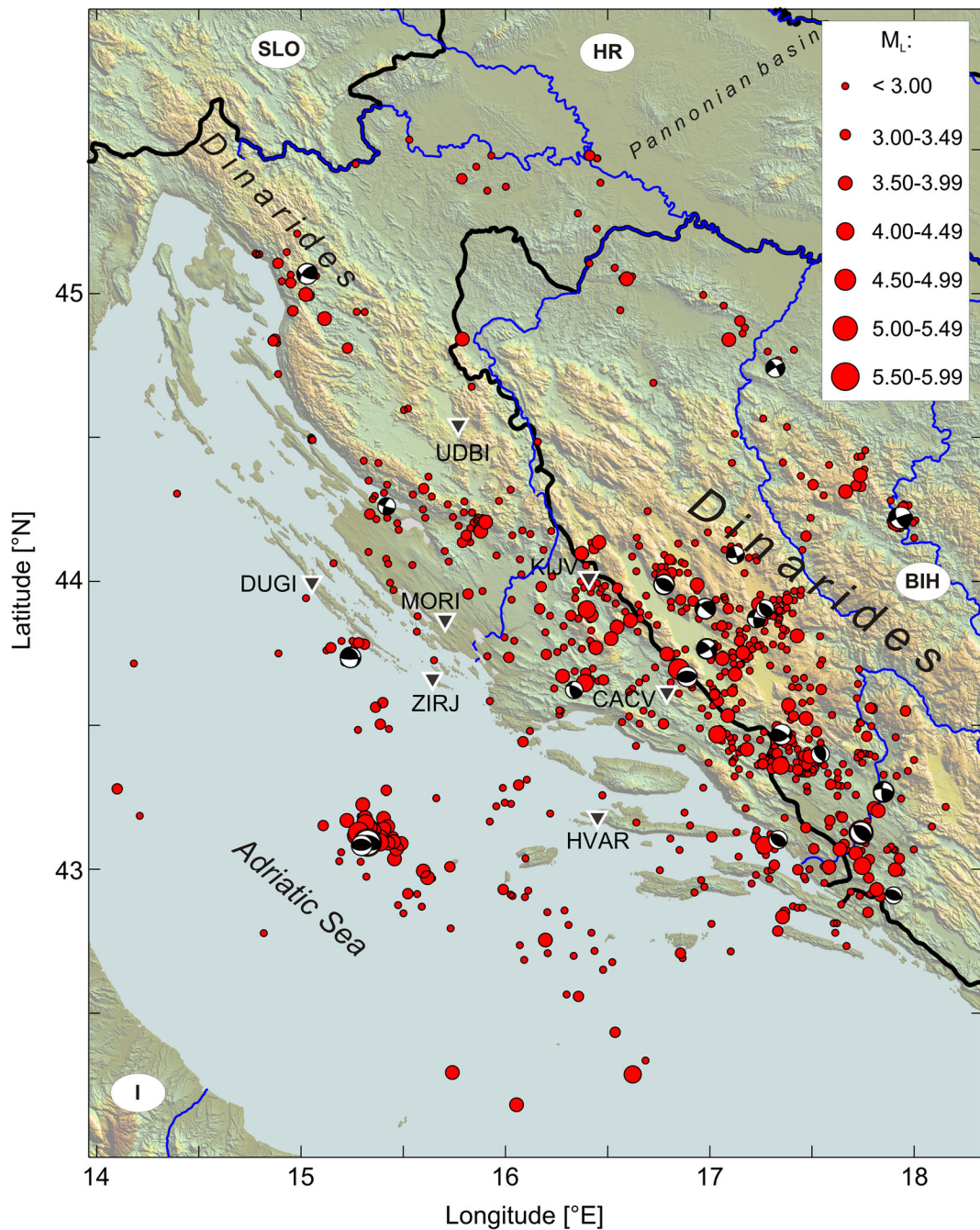


**Fig. 2** Seismological stations (*triangles*) and epicentres of earthquakes (*circles*) used. Earthquakes for which the fault plane solution is known are marked by corresponding *beach ball diagrams*

the normalizing window is in the coda wavetrain and  $SNR$  is favourable even for weak, distant earthquakes: for most earthquakes,  $t_C > 2t_S$  and always  $t_C > 1.5t_S$ .

For each central frequency, possible outliers were discarded from the sample. Outliers were defined as values out of range  $[q_1 - a \cdot iqr, q_3 + a \cdot iqr]$ , where  $q_1$

and  $q_3$  are the lower and the upper quartiles,  $iqr$  is the interquartile range of  $\ln \frac{A_p \cdot s(f) \cdot r}{A_c(f, t_C)}$  for each of the 10-km-wide classes of hypocentral distances,  $a=1.1$  for P-waves and  $a=1.5$  for S-waves. Ordinary least squares method was used for the linear regression (Eq. 1); from the slope of the regression line  $b$  (Fig. 4), we calculated

**Table 1** Instruments, sampling frequency  $f_s$  and time interval in which considered events occurred

Station	Instruments	$f_s$ (sps)	Time interval	$N$
Udbina (UDBI)	Güralp CMG-40T	50	2009–2013	112
Kijevo (KIJV)	Güralp CMG-40T	50	2007–2013	246
Čačvina (CACV)	Güralp CMG-40T	50	2007–2013	238
Morići (MORI)	Güralp CMG-40T	50	2011–2013	125
Dugi Otok (DUGI)	Güralp CMG-40T	50	2011–2013	59
Žirje (ZIRJ)	Güralp CMG-40T	50	2011–2013	137
Hvar (HVAR)	Güralp CMG-40T, STS-2	40, 50, 100	2001–2013	282

$N$  is the number of analyzed seismograms

$Q_P(f) = -\frac{\pi f}{b_P v_P}$  and  $Q_S(f) = -\frac{\pi f}{b_S v_S}$ , assuming  $v_P = 5.80$  km/s and  $v_S = 3.45$  km/s in agreement with Herak and Herak (1995). After  $Q_P$  and  $Q_S$  were obtained for each central frequency,  $Q_{0,P} = Q_P(f=1 \text{ Hz})$  and  $Q_{0,S} = Q_S(f=1 \text{ Hz})$  along with the frequency dependence exponents  $n_P$  and  $n_S$  in Eq. (2) were estimated by applying the robust linear regression (iteratively reweighted least squares method with bisquared weighting function).

Described procedures are applied to each station's data set independently and to the set that consists of all the data together denoted as CED.

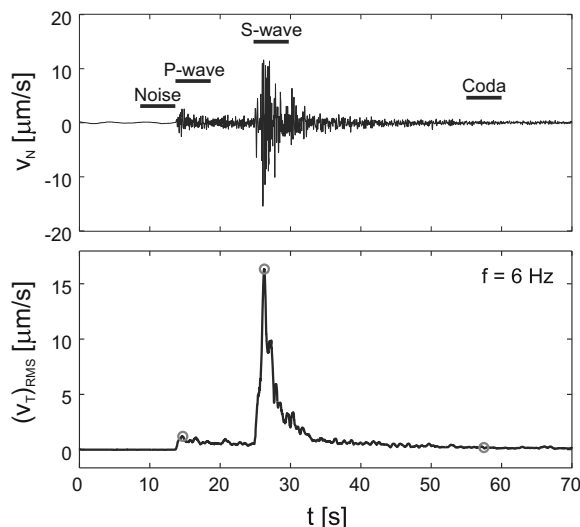


**Fig. 3** Example of the procedure applied to the seismogram of a local earthquake that occurred on 19 April 2013 at 08:49:13.7,  $M = 2.6$  and  $\Delta = 83$  km, recorded at station MORI. *Top*: N–S component of the seismogram with horizontal bars indicating positions and lengths of time windows used in the analysis. *Bottom*: root-mean-square (RMS) envelope of the total velocity field for band-pass-filtered signal for  $f = 6$  Hz. Circles denote the amplitudes used in the analysis (Eq. 1)

#### 4 Results and discussion

Obtained values for  $Q_P(f)$  and  $Q_S(f)$  are presented in Fig. 5. For low frequencies,  $Q_P$  is consistently lower for the island stations than for stations located on mainland, whereas there is no prominent difference in attenuation of S-waves, except at the most outward station HVAR for intermediate and high frequencies. The minimum values of  $Q_P$  and  $Q_S$  are 32 and 60, respectively, at  $f = 1.5$  Hz obtained for the station DUGI, whereas the largest  $Q$ -values of  $Q_P = 1089$  and  $Q_S = 1707$  are observed for HVAR at  $f = 24$  Hz. The results, of course, depend on the choice of the average velocities  $v_P$  and  $v_S$  in the upper crust. However, the variation of  $Q$ -factors due to the uncertainty and/or spatial variation of velocities are small and within their estimated confidence levels. Standard errors are larger for P-waves than for S-waves, especially at the lowest considered frequencies of 1.5 and 2 Hz; scatter of the data for these frequencies are larger, and the sets are smaller due to often unfavourable signal to noise ratios. High level of ambient noise at low frequencies is most probably caused by the sea waves and strong winds that are common there.

Frequency dependence is pronounced for all stations and both types of body waves (Table 2):  $n_P = 0.56\text{--}1.52$  and  $n_S = 0.65\text{--}0.97$ .  $Q_{0,P}$  ranges between 21 at DUGI and 120 at CACV, whereas  $Q_{0,S}$  is between 46 at UDBI and 113 at KIJV. The results for the area as a whole (CED) are  $Q_P(f) = 75f^{0.75}$  and  $Q_S(f) = 96f^{0.69}$ . These results are close to what was found in studies related to the neighbouring areas. For Umbria–Marche region, Italy, de Lorenzo et al. (2013) obtained  $Q_S = (25 \pm 4) f^{0.99 \pm 0.02}$ . There are estimations of body wave attenuation calculated using the nonparametric attenuation functions in Slovenia and Italy. Kastelic et al. (2010) obtained  $Q_S = 83f^{0.80}$  for western and central Slovenia. Castro

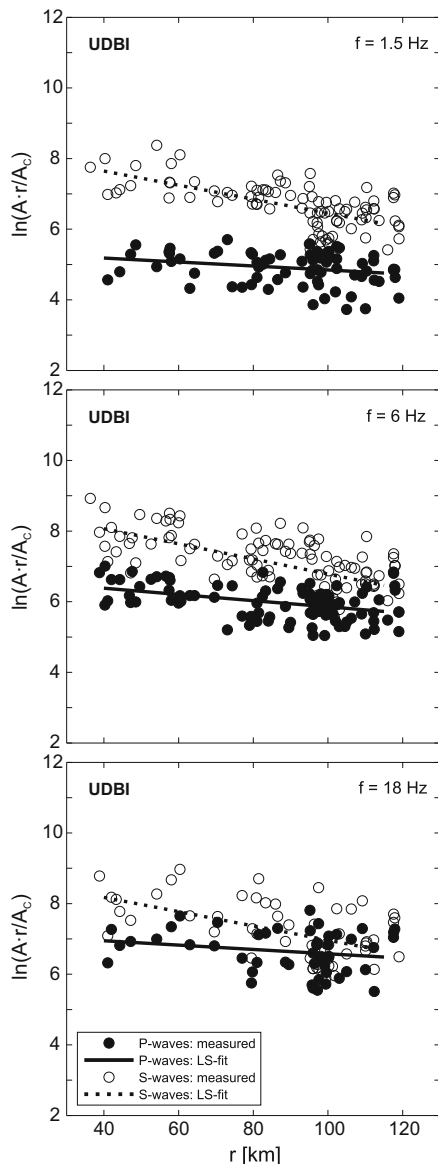


**Fig. 4** Plots of the logarithm of the normalized spectral amplitudes against hypocentral distance for P- and S-waves for three central frequencies.  $Q_P(f)$  and  $Q_S(f)$  are calculated from the slope of the regression line. Example for the station UDBI

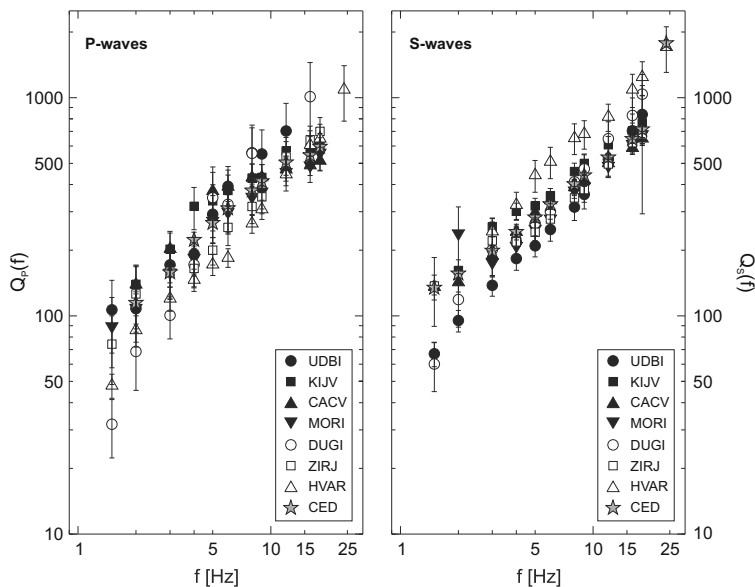
et al. (1996) estimated  $Q_S=16f^{0.92}$  from accelerograms for the Friuli region in NE Italy. For the region of Garda, Castro et al. (2008) reported  $Q_P=65f^{0.9}$  and  $Q_S=160f^{0.6}$ . For Marche in Italy, Castro et al. (1999) evaluated  $Q$ -factors for P-, SV- and SH-waves from accelerograms:  $Q_P=108.4f^{0.70}$ ,  $Q_{SV}=105.6f^{0.65}$  and  $Q_{SH}=86.1f^{0.70}$ . In the same manner, Polatidis et al. (2003) determined the S-wave attenuation for back-arc region of the Hellenic arc as  $Q_S=55f^{0.91}$ . Tselentis (1998) calculated  $Q_S$

(1 Hz)=119 applying the approach proposed by Tsujiura (1966) to Western Greece. In Northern Greece, Hatzidimitriou (1995) obtained  $Q_S=(85\pm 1)f^{0.91\pm 0.07}$  by applying the coda normalization method. In the Sea of Marmara, Turkey, Horasan and Boztepe-Güney (2004) estimated  $Q_S=(40\pm 5)f^{1.03\pm 0.06}$ .

Numerous studies have shown that  $Q_S/Q_P$  ratio can give some insight into attenuation mechanisms: scattering, pore fluid content, confining pressure or the relative change in elastic moduli may dramatically affect the ratio. Winkler and Nur (1979) suggest that  $Q_S/Q_P$  is better indicator of rock fluid content than  $v_P/v_S$ . Laboratory experiments showed that partially saturated rocks have  $Q_S/Q_P > 1$  whereas for total saturation and dry rock  $Q_S/Q_P < 1$  (ultrasonic and acoustic frequency range; Toksöz et al. 1979; Winkler and Nur 1982). According to Adam et al. (2009) and references therein, results obtained for carbonates suggest that, in general,  $Q_P < Q_S$  for  $f=10-100$  Hz and that the attenuation is sensitive to the type of the fluid (e.g. brine or hydrocarbon), fluid flow and the size of pores. Their research shows that P-wave attenuation increases ( $Q_P$  decreases) notably when brine replaces light hydrocarbon in the pores. A thorough review of research on the influence of various parameters on attenuation of seismic waves was published by Barton (2007). Hough and Anderson (1988) pointed out that, in general,  $Q_S/Q_P \geq 1$  for most kinds of scattering. According to Padhy (2009), high values of the ratio  $Q_S/Q_P$  are expected when there is notable scattering from shallow heterogeneities in the crust.

Let us look at the  $Q_S/Q_P$  ratio at different frequencies in Fig. 6. For almost all stations, the ratio has values between 0.55 and 1.40. For the area as a whole, the ratio is between 1.0 and 1.4. Only for the most NW station UDBI, which is located in a low-seismicity region, in the hinterlands of Mt. Velebit, the ratio is consistently less than 1; i.e. P-waves are somewhat less attenuated than S-waves ( $Q_S < Q_P$ ). For the rest of continental stations (KIJV, CACV and MORI)  $Q_S/Q_P \approx 1$ : they differ for  $f < 5$  Hz, but for intermediate and high frequencies, the ratios are very similar and increase slightly with frequency. The ratios for island stations DUGI and ZIRJ are high ( $> 1.5$ ) at low frequencies, but below 1 at high frequencies ( $f > 10$  Hz). The smallest difference between all stations is at intermediate frequencies ( $Q_S/Q_P \approx 1$ ) except for HVAR which differs considerably from all other stations: values of the ratios are very high exceeding 2.0 ( $Q_S/Q_P=2.75$  at  $f=6$  Hz). This means that

**Fig. 5** Frequency distribution of estimated  $Q_P$  (left) and  $Q_S$  (right). Solid symbols denote inland stations, and empty ones stand for island stations. Error bars describe standard error



attenuation in the area surrounding HVAR is much stronger for P-waves than for S-waves. Being the most outward station of all, a large proportion of raypaths considered lie largely or even entirely within the Adriatic microplate. This result may therefore indicate fundamental difference of attenuation properties of the two major tectonic units. Furthermore, as noted above, a large portion of HVAR seismograms are of the earthquakes in the Jabuka Island region in the middle of the Adriatic sea, which is a Triassic igneous body extruded by the diapir tectonics with the ongoing halokinetic activity (Pikelj et al. 2015). This may indicate that pores in the large region around the epicentral area are partially saturated with saltwater at seismogenic depths, thus strongly influencing body wave attenuation (Adam et al. 2009; Winkler and Nur 1982). Salt intrusions may also enhance backscattering, which would in turn increase

the scattering component of attenuation. This would be consistent with the observed  $Q_S > Q_P$  which is an indication that scattering  $Q$  dominates over intrinsic  $Q$  in total attenuation (Kang and McMechan 1994; Padhy 2009). The Jabuka area is also characterized by higher temperatures and higher heat flow than the neighbouring regions (see the discussion below). In general, the attenuation of P-waves is slightly stronger than S-wave attenuation, more noticeably at low frequencies; in terms of scattering, this would imply notable scattering of S-waves in the crust. Regarding the intrinsic attenuation and its diverse mechanisms, and in

**Table 2** Estimated values for  $Q_P$  (1 Hz),  $Q_S$  (1 Hz),  $n_P$  and  $n_S$

Station	$Q_{0,P} \pm \sigma$	$n_P \pm \sigma$	$Q_{0,S} \pm \sigma$	$n_S \pm \sigma$
UDBI	58±7	1.03±0.08	46±2	0.97±0.03
KIJV	110±15	0.63±0.07	113±7	0.67±0.03
CACV	120±23	0.56±0.09	98±4	0.66±0.02
MORI	69±5	0.75±0.04	73±7	0.77±0.05
DUGI	21±5	1.52±0.14	59±4	0.95±0.04
ZIRJ	55±5	0.87±0.05	96±9	0.65±0.04
HVAR	34±3	1.03±0.04	98±7	0.89±0.03
CED	75±6	0.75±0.04	96±7	0.69±0.04

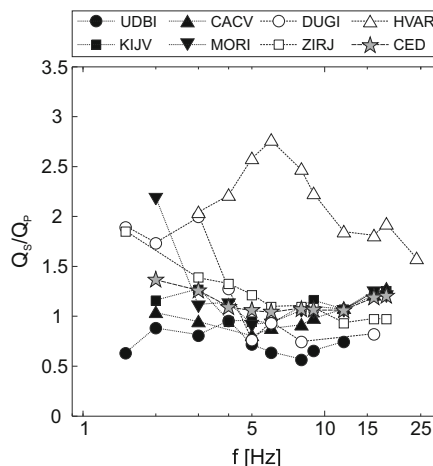


**Fig. 6** Ratio  $Q_S(f)/Q_P(f)$  for different frequencies. Solid symbols mark inland stations, and empty symbols stand for island stations



light of previous discussion, results may suggest mostly partially saturated rocks.

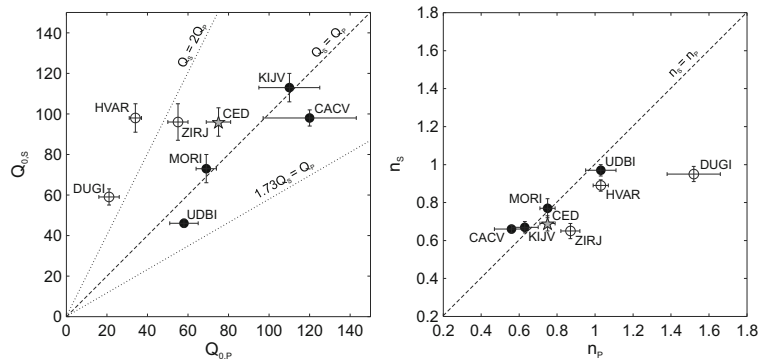
There are several studies for various regions of the world that have considered  $Q_S/Q_P$ , and most of them report the ratio  $Q_S/Q_P > 1$  for all frequencies. Castro et al. (2008) found  $Q_S/Q_P$  to be between 0.7 and 2.8 for the region of Garda, the Central Alps, which is in an excellent agreement with results presented here. Yoshimoto et al. (1993) estimated  $Q_S/Q_P > 1$  for Kanto region, Japan, whereas Mahood et al. (2009) obtained ratios between 1.3 and 2.0 in East Central Iran. For Garhwal Himalaya, Tripathi et al. (2014) calculated  $Q_S/Q_P = 1.6–3.0$ ; Singh et al. (2012) estimated  $Q_S/Q_P = 3.9–4.8$  for Kamaun Himalaya and, for Kinnaur Himalaya,  $Q_S/Q_P = 1.5–1.8$  (Kumar et al. 2014). Chung and Sato (2001) obtained  $Q_S/Q_P = 1.1–2.8$  for more stable SE South Korea. The frequency trends are very diverse, different for each studied area. In a comprehensive study of the frequency-independent crustal attenuation in southern California, Hauksson and Shearer (2006) obtained the mean value of  $Q_S/Q_P$  equal to 1.3, which they interpreted as indication of partial saturation of crustal rocks with pore fluids. They attribute isolated cases of  $Q_S/Q_P < 1$  to elevated crustal temperatures, high fluid saturation or a larger reduction in the shear modulus compared to the bulk modulus.

When quality factors at 1 Hz for P- and S-waves,  $Q_{0,P}$  and  $Q_{0,S}$ , are compared, we see that their ratios vary with location of the corresponding stations (Fig. 7). The stations situated on islands (empty circles in Fig. 7), next to the border with the Adriatic microplate, have  $Q_{0,S}$  about twice as large as  $Q_{0,P}$  whereas stations well in the Dinarides (solid circles in Fig. 7) have  $Q_{0,S}$  equal or less than  $Q_{0,P}$ . Frequency dependence exponents  $n$  for P- and S-waves are almost equal for inland stations, but for island stations,  $n_P$  is larger than  $n_S$ .

The two groups are far from homogeneous, especially when absolute attenuation and details of frequency dependence of  $Q$  are considered. For instance, as noted above, HVAR stands out by very large  $Q_S(f)/Q_P(f)$  for all frequencies. UDBI—situated in the low-seismicity Mt. Velebit karst region, perhaps the most puzzling area of the External Dinarides characterized by a possible contemporary seismic gap—is distinguished within its group by the lowest  $Q_P$  and  $Q_S$  and is the only station with  $Q_S(f)/Q_P(f) < 1$ , regardless of frequency. On the other hand, the stations KIJV and CACV located in the area where seismicity is high and the crust is the thickest exhibit comparatively low attenuation at 1 Hz ( $Q_{0,P}, Q_{0,S} > 95$ ) and the weakest frequency dependence ( $n_P, n_S < 0.70$ ), which may indicate that the share of scattering  $Q$  in total attenuation is smaller than elsewhere (e.g. Kang and McMechan 1994).

Attenuation is more sensitive to the heat than are the seismic velocities: velocity depends nearly linearly on temperature, whereas attenuation shows exponential dependence on temperature (Stein and Wysession 2003). The lowest formation temperatures and heat flows are reported for the Split-Sinj area:  $\leq 30^\circ\text{C}$  at 2000-m depth and  $\leq 20\text{ mW/m}^2$  (Jelić et al. 1995) and  $\leq 30^\circ\text{C}$  at 3000-m depth (Grandić et al. 2010). The highest formation temperatures and heat flows are found in the area of Jabuka Island:  $\geq 60^\circ\text{C}$  at 2000-m depth and  $\geq 35\text{ mW/m}^2$  (Jelić et al. 1995) and  $60–70^\circ\text{C}$  at 3000-m depth (Grandić et al. 2010). Area west of Dugi Otok Island also stands out with temperatures  $50–60^\circ\text{C}$  at 3000-m depth (Grandić et al. 2010) and  $\geq 60^\circ\text{C}$  at 2000-m depth (Jelić et al. 1995). Lenkey et al. (2002) reported on the heat flow: it is  $\approx 30\text{ mW/m}^2$  for the most of the area,  $40\text{ mW/m}^2$  along Dugi Otok–Vis to more than  $50\text{ mW/m}^2$  NW of Zadar. In the thermal model of European lithosphere Tesauro et al. (2009) indicated increase in

**Fig. 7** Relations between  $Q_{0,P}$  and  $Q_{0,S}$  (left) and  $n_P$  and  $n_S$  (right). Error bars stand for standard error. Solid circles represent mainland stations, and empty circles denote island stations



depth of 1200 °C–isotherm (lithosphere–asthenosphere boundary) from 130–140 to 150–160 km from NE, NW and SW towards the CED. Comparison of these thermal characteristics with the results of this study shows that higher  $Q_P$  factors, i.e. lower P-wave attenuation, are estimated at stations in areas with lower temperatures and low heat flow, whereas lower  $Q_P$  values are found in areas with higher temperatures and high heat flow. Furthermore, the stations with lower  $Q_P$  values are in the area of high  $v_P$  in the upper crust (Herak and Herak 1995). These relations are not that straightforward for S-waves: for ZIRJ and HVAR, we would expect lower values, compared to other stations.

Dasović et al. (2012, 2013) estimated coda- $Q$  attenuation for stations UDBI, KIJV, CACV, DUOK (DUGI) and HVAR by applying coda- $Q$  method proposed by Aki and Chouet (1975) for different parts of coda defined by the lapse time  $t_L$ , i.e. the time elapsed since the origin time. Comparison of their  $Q_{0,C}=Q_C$  (1 Hz) with  $Q_{0,S}$  obtained in this analysis is presented in Fig. 8. It should be mentioned that more earthquakes were used here for the S-wave analysis than for the study of attenuation of coda waves. Moreover, DUGI and DUOK are two different stations on the island of Dugi Otok, which operated at different times and at different locations: DUOK was operational in the years 2000–2001 (van der Lee et al. 2001) around 17 km NNW from DUGI which operates since 2011. Keeping this in mind, we can conclude that overall attenuation of direct S-waves is larger than attenuation of the coda waves. In the earliest part of coda ( $t_L=30$  s), corresponding mostly to scattering within the crust, at KIJV, CACV and HVAR, the  $Q$ -factors are almost equal, but  $Q_{0,C}/Q_{0,S}$  increases as the  $t_L$  increases. This indicates that direct body waves and the scattered waves constituting early coda are attenuated there by similar mechanisms.

Ratio of frequency dependence exponents for coda and S-waves is between 0.51 and 1.35; as lapse time increases, coda- $Q$  weakens its frequency dependence, i.e.  $n_C/n_S$  decreases. Coda- $Q$  is a result of a complex interaction of intrinsic and scattering attenuation. Higher  $Q_C$  in later part of coda is interpreted as being caused by, on average, less-attenuated backscattered waves coming from larger depths where intrinsic  $Q$ -factor is higher. Moreover, in its later parts, multiple scattering becomes important causing more energy to be distributed back into coda. This is especially important at high frequencies and is known as the high-frequency coda enrichment (Padhy and Subhadra 2010). In the work of Padhy

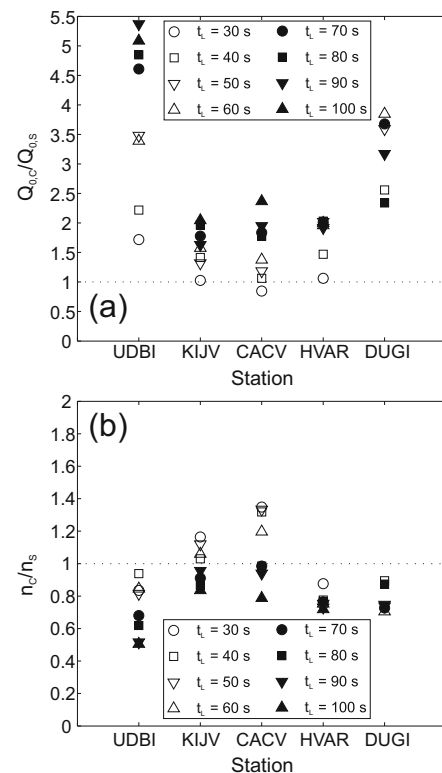


**Fig. 8** Comparison of  $Q_{0,C}=Q_C$  (1 Hz) obtained in previous studies (Dasović et al. 2012, 2013) with  $Q_{0,S}$  (a) and ratio of frequency dependence parameter for coda and S-waves (b). Coda- $Q$ -factor was estimated for different parts of coda:  $t_L$  represents the lapse time of a middle of the 30-s-long coda window that was analyzed

and Subhadra (2010) for NE India,  $Q_{0,C}$  is at least twice as high as  $Q_{0,S}$  and  $n_C < n_S$ . De Lorenzo et al. (2013) report  $Q_{0,C}/Q_{0,S} > 2.5$  and  $n_C < n_S$  for Umbria–Marche region in Italy. Mahood and Hamzehloo (2011) showed that in East Central Iran,  $Q_{0,C}/Q_{0,S} > 1.2$  and  $n_C \approx n_S$ . Results obtained in this study for the CED indicate that scattering of direct S-waves could also be notable, indicating heterogeneous upper crust. However, for better distinction of intrinsic and scattering attenuation, other techniques should be applied (for example, Wennerberg 1993 or MLTWA method explained in Sato et al. 2012).

## 5 Conclusions

We estimated quality factors of high-frequency body waves by applying extended coda normalization method to seismograms of seven seismological broadband

stations in the area of the CED. The analysis of local earthquakes shows that this seismically active and tectonically complex area highly attenuates both P- and S-waves. P-waves, in general, lose more energy on their path than S-waves ( $Q_P < Q_S$ ): obtained  $Q_P$  (1 Hz) values range from 21 to 120, while for  $Q_S$  (1 Hz), values from 46 to 113 are found. The exponent controlling the frequency dependence of  $Q$ -factors in the simple power law ranges from 0.63 to 1.52 for  $n_P$  and from 0.65 to 0.97 for  $n_S$ .

From the analyses above, we can roughly differentiate between two types of attenuation properties. The first one is characteristic of the island stations DUGI, ZIRJ and HVAR. They distinguish themselves by the strong low-frequency P-wave attenuation and more pronounced frequency dependence of the  $Q_P$  factor ( $Q_{0,S}/Q_{0,P} > 1.7$ ,  $Q_{0,P} < 60$ ,  $n_P > n_S$ ). Hence, although attenuation is larger for P-waves than for S-waves near 1 Hz, as frequency increases, S-waves tend to attenuate more relative to the P-waves. The second group is formed by the four stations (UDBI, MORI, KIJV, CACV) situated on the mainland, which all exhibit similar attenuation properties for P- and S-waves ( $n_P \approx n_S \approx 1$  and  $Q_{0,S} \approx Q_{0,P}$ ).

The results are qualitatively in agreement with the thermal regime in the area. Comparison of thermal characteristics of the greater region of CED with the results from this study shows that the highest  $Q_P$  factors (CACV, KIJV) are estimated at stations in areas with low temperatures and low heat flow, whereas the lowest  $Q_P$  (at the three island stations) corresponds to areas with higher temperatures and high heat flow. Furthermore, the stations with lower  $Q_P$  values are located in the area of increased  $v_P$  in the upper crust.

At low frequency, attenuation of direct S-waves in the crust is stronger than attenuation of scattered coda waves in the lithosphere, especially for later parts of coda, i.e. larger lapse times.

**Acknowledgments** We thank the two anonymous reviewers for their constructive criticism of the manuscript. We also thank the Croatian Seismological Survey for the use of the data. We gratefully acknowledge the financial support from the Ministry of Science, Education and Sports of the Republic of Croatia, grants 119-1193086-1315 and 119-1193086-1314, and annual research subsidy grants from the University of Zagreb.

**Conflict of interest** The authors declare that they have no conflict of interest.

## References

- Adam L, Batzle M, Lewallen KT, van Wijk K (2009) Seismic wave attenuation in carbonates. *J Geophys Res* 114, B06208. doi:10.1029/2008JB005890
- Aki K (1980) Attenuation of shear-waves in the lithosphere for frequencies from 0.05 to 25 Hz. *Phys Earth Planet Inter* 21: 50–60
- Aki K, Chouet B (1975) Origin of coda waves: source, attenuation, and scattering effects. *J Geophys Res* 80:3322–3342
- Barton N (2007) Rock quality, seismic velocity, attenuation and anisotropy. Taylor & Francis Group, London
- Castro RR, Pacor F, Sala A, Petrongaro C (1996) S wave attenuation and site effects in the region of Friuli, Italy. *J Geophys Res* 101:22355–22369
- Castro RR, Monarchesi G, Mucciarelli M, Trojani L, Pacor F (1999) P- and S-wave attenuation in the region of Marche, Italy. *Tectonophysics* 302:123–132
- Castro RR, Massa M, Augliera P, Pacor F (2008) Body-wave attenuation in the region of Garda, Italy. *Pure Appl Geophys* 165:1351–1366. doi:10.1007/s00024-008-0365-1
- Chung T-W, Sato H (2001) Attenuation of high-frequency P and S waves in the crust of Southeastern South Korea. *Bull Seismol Soc Am* 91:1867–1874
- Dasović I, Herak M, Herak D (2012) Attenuation of coda waves in the contact zone between the Dinarides and the Adriatic Microplate. *Stud Geophys Geod* 56:231–247. doi:10.1007/s11200-010-0077-8
- Dasović I, Herak M, Herak D (2013) Coda-Q and its lapse time dependence analysis in the interaction zone of the Dinarides, the Alps and the Pannonian basin. *J Phys Chem Earth* 63:47–54. doi:10.1016/j.pce.2013.03.001
- De Lorenzo S, Del Pezzo E, Bianco F (2013)  $Q_c$ ,  $Q_\beta$ ,  $Q_i$  and  $Q_s$  attenuation parameters in the Umbria-Marche (Italy) region. *Phys Earth Planet Inter* 218:19–30. doi:10.1016/j.pepi.2013.03.002
- Grandić S, Kratković I, Rusan I (2010) Hydrocarbon potential assessment of the slope deposits along the SW Dinarides carbonate platform edge. *Nafta* 61:325–338
- Hatzidimitriou PM (1995) S-wave attenuation in the crust in Northern Greece. *Bull Seism Soc Am* 85:1381–1387
- Hauksson E, Shearer PM (2006) Attenuation models ( $Q_P$  and  $Q_S$ ) in three dimensions of the southern California crust: inferred fluid saturation at seismogenic depths. *J Geophys Res* 111, B05302. doi:10.1029/2005JB003947
- Havskov J, Ottemöller L (2010) Routine data processing in earthquake seismology. Springer, Science+Business Media B.V
- Herak M (1991) Lapse time dependent  $Q_c$ -spectra observed in the Dinarides region (Yugoslavia). *Phys Earth Planet Inter* 67: 303–312
- Herak D, Herak M (1995) Body-wave velocities in the circum-Adriatic region. *Tectonophysics* 241:121–141
- Herak M, Herak D, Markušić S (1996) Revision of the earthquake catalogue and seismicity of Croatia, 1908–1992. *Terra Nova*. 8:86–94
- Herak D, Herak M, Prelogović E, Markušić S, Markulin Ž (2005) Jabuka island (Central Adriatic Sea) earthquakes of 2003. *Tectonophysics* 398:167–180. doi:10.1016/j.tecto.2005.01.007
- Herak M, Allegretti I, Herak D, Ivančić I, Kuk V, Marić K, Markušić S, Sović I (2011) Republika Hrvatska, Karta

- potresnih područja (Republic of Croatia, Seismic Hazard Maps; in Croatian). University of Zagreb, Faculty of Science, Department of Geophysics. <http://seizkarta.gfz.hr/karta.php>. Accessed 19 December 2014. In: Eurocode 8: design of structures for earthquake resistance—part 1: general rules, seismic actions and rules for buildings. National Annex. Croatian Standards Institute, pp 28
- Horasan G, Boztepe-Güney A (2004) S-wave attenuation in the Sea of Marmara, Turkey. *Phys Earth Planet Inter* 14:215–224. doi:10.1016/j.pepi.2004.01.004
- Hough SE, Anderson JG (1988) High-frequency spectra observed at Anza, California: implications for Q structure. *Bull Seismol Soc Am* 78:692–707
- Ivančić I, Herak D, Markušić S, Sović I, Herak M (2006) Seismicity of Croatia in the period 2002–2005. *Geofizika* 23:87–103
- Jelić K, Kevrić I, Krsić O (1995) Temperatura i toplinski tok u tlu Hrvatske. *Proc First Croat Geol Congr, Opatija, Croatia* 1: 245–249
- Kang IB, McMechan GA (1994) Separation of intrinsic and scattering Q based on frequency-dependent amplitude ratios of transmitted waves. *J Geophys Res* 99:23875–23885
- Kastelic V, Kiratzi A, Benetatos C, Živčić M, Bajc J (2010) Shear wave Q determination for the upper crust of the western and central Slovenia. *Sci Ann Sch Geol Univ Thessaloniki, Proc XIX CBGA Congr, Spec volume* 99:377–385
- Kuk V, Prelogović E, Dragičević I (2000) Seismotectonically active zones in the Dinarides. *Geol Croat* 53:295–303
- Kumar N, Shonkholen M, Mukhopadhyay S (2014) Estimation of  $Q_p$  and  $Q_s$  of Kinnaur Himalaya. *J Seismol* 18:47–59. doi:10.1007/s10950-013-9399-7
- Lenkey L, Dövényi P, Horváth F, Cloetingh SAPL (2002) Geothermics of the Pannonian basin and its bearing on the neotectonics. *EGU Stephan Mueller Spec Publ Series* 3:29–40
- Mahood M, Hamzehloo H (2011) Variation of intrinsic and scattering attenuation of seismic waves with depth in the Bam region, East-Central Iran. *Soil Dyn Earthq Eng* 31:1338–1346. doi:10.1016/j.soildyn.2011.05.010
- Mahood M, Hamzehloo H, Doloei GJ (2009) Attenuation of high frequency P and S waves in the crust of the East-Central Iran. *Geophys J Int* 179:1669–1678. doi:10.1111/j.1365246X.2009.04363.x
- Markušić S, Herak M (1999) Seismic zoning of Croatia. *Nat Hazards* 18:269–285
- Padhy S (2009) Characteristics of body-waves attenuations in the Bhuj crust. *Bull Seismol Soc Am* 99:3300–3313. doi:10.1785/0120080337
- Padhy S, Subhadra N (2010) Attenuation of high-frequency seismic waves in northeast India. *Geophys J Int* 181:453–467. doi:10.1111/j.1365-246X.2010.04502.x
- Pikelj K, Hermitz-Kučenjak M, Aščić Š, Juračić M (2015) Surface sediment around the Jabuka Islet and the Jabuka Shoal: evidence of Miocene tectonics in the Central Adriatic Sea. *Mar Geol* 359:120–133. doi:10.1016/j.margeo.2014.11.003
- Polatidis A, Kiratzi A, Hatzidimitriou P, Margaris B (2003) Attenuation of shear-waves in the back-arc region of the Hellenic arc for frequencies from 0.6 to 16 Hz. *Tectonophysics* 367:29–40. doi:10.1016/S0040-1951(03)00136-7
- Sato H, Fehler MC, Maeda T (2012) Seismic wave propagation and scattering in the heterogeneous earth: second edition. Springer-Verlag, Heidelberg
- Singh C, Singh A, Srinivasa Bharathi VK, Bansal AR, Chadha RK (2012) Frequency-dependent body wave attenuation characteristics in the Kumaun Himalaya. *Tectonophysics* 524–525: 37–42. doi:10.1016/j.tecto.2011.12.013
- Stein S, Wysession M (2003) An introduction to seismology, earthquakes, and earth structure. Blackwell Publishing, Oxford
- Stipčević J (2012) Crustal and upper mantle structure beneath the Dinarides determined from broadband receiver function. Dissertation (in Croatian with English abstract), Faculty of Science, University of Zagreb
- Stipčević J, Tkaličić H, Herak M, Markušić S, Herak D (2011) Crustal and uppermost mantle structure beneath the External Dinarides, Croatia, determined from teleseismic receiver functions. *Geophys J Int* 185:1103–1119. doi:10.1111/j.1365-246X.2011.05004.x
- Tesauro M, Kaban MK, Cloetingh SAPL (2009) A new thermal and rheological model of the European lithosphere. *Tectonophysics* 476:478–495. doi:10.1016/j.tecto.2009.07.022
- Toksöz MN, Johnston DH, Timur A (1979) Attenuation of seismic waves in dry and saturated rocks: I Laboratory measurements. *Geophysics* 44:681–690
- Tomljenović B, Csontos L, Márton E, Márton P (2008) Tectonic evolution of the northwestern Internal Dinarides as constrained by structures and rotation of Medvednica Mountains, North Croatia. In: Siegesmund S, Fügenschuh B, Froitzheim N (eds) Tectonic aspects of the Alpine-Dinaride-Carpathian system. *Geol Soc Lond Spec Publ*, 298:145–167. doi:10.1144/SP298.8
- Tripathi JN, Priyamvada S, Sharma ML (2014) Attenuation of high-frequency P and S waves in Garhwal Himalaya, India. *Tectonophysics* 636:216–227. doi:10.1016/j.tecto.2014.08.015
- Tselentis GA (1998) Intrinsic and scattering seismic attenuation in W. Greece. *Pure Appl Geophys* 153:703–712
- Tsujiura M (1966) Frequency analysis of the seismic waves, I. *Bull Earthq Res Inst Tokyo Univ* 44:873–891
- Ustaszewski K, Schmid SM, Fügenschuh B, Tischler M, Kissling E, Spakman W (2008) A map-view restoration of the Alpine-Carpathian-Dinaridic system for the Early Miocene. *Swiss J Geosci* 101:S273–S294. doi:10.1007/s00015-008-1288-7
- Van der Lee S, Marone F, van der Meijde M, Giardini D, Deschamps A, Margheriti L, Burkett P, Solomon SC, Alves PM, Chouliaras M, Eshwedi A, Suleiman AS, Gashut H, Herak M, Ortiz R, Davila JM, Aguirre A, Vila J, Yelles K (2001) Eurasia-Africa plate boundary region yields new seismographic data. *EOS Trans AGU* 82:637–646
- Wennerberg L (1993) Multiple scattering interpretation of coda Q measurements. *Bull Seismol Soc Am* 83:279–290
- Winkler K, Nur A (1979) Pore fluids and seismic attenuation in rocks. *Geophys Res Lett* 6:1–4. doi:10.1029/GL006i001p00001
- Winkler KW, Nur A (1982) Seismic attenuation: effects of pore fluids and frictional sliding. *Geophysics* 47:1–15. doi:10.1190/1.1441276
- Yoshimoto K, Sato H, Ohtake M (1993) Frequency-dependent attenuation of P and S waves in the Kanto area, Japan, based on the coda-normalization method. *Geophys J Int* 114:165–174